ORIGINAL ARTICLE

Thermoelectric properties of zigzag single-walled Carbon nanotubes and zigzag single-walled Boron Nitride nanotubes (9, 0)

Reza Sadeghi, Mohammad Reza Niazian*, Mojtaba Yaghobi, Mohammad Ali Ramzanpour

Department of Physics, Ayatollah Amoli Branch, Islamic Azad University, Amol 46351-43358, Iran

Abstract
In this paper, the thermoelectric properties of zigzag single-walled carbon nanotubes (SWCNT) and zigzag single-walled boron nitride nanotubes (SWBNNT) are investigated. For this purpose, the chirality is considered as (9, 0). The characteristics are computed at three arbitrary temperatures of 200K, 300K, and 500K. Results show the Seebeck coefficient of zigzag SWCNT increases by increasing the temperature, while decreases for the zigzag SWBNNT. The peak of the Seebeck coefficient of the zigzag SWCNT at the temperatures of 200K, 300K, and 500K are $4.97\times10^{-5}\left(\frac{V}{K}\right)$, $4.88\times10^{-5}\left(\frac{V}{K}\right)$, and $5.70\times10^{-5}\left(\frac{V}{K}\right)$, respectively. The associated values of SWBNNT are, $4.38\times10^{-3}\left(\frac{V}{K}\right)$, $3.03\times10^{-3}\left(\frac{V}{K}\right)$ and $2.0\times10^{-3}\left(\frac{V}{K}\right)$, respectively. Besides, it is observed that at the temperature of 200K, the Seebeck coefficient zigzag SWBNNT is about 88 times the value of zigzag SWCNT. Moreover, due to the Seebeck coefficient sign type in the Fermi energy range, both of the considered nanostructures are semiconductors and n-type. It is depicted that the electrical conductivity and total thermal conductance of SWCNT are larger than SWBNNT. Efficiency is an important parameter to characterize the thermoelectric properties of nanomaterials. Results show the figure-of-merit (ZT) value of SWBNNT is much better than that of SWCNT. Due to the contribution of phonons, the zigzag SWBNNT has larger Seebeck coefficient. The studies show that the maximum value of ZT of the zigzag SWBNNT at the temperatures of 200K, 300K and, 500K are larger than 0.0207, 0.0342 and, 0.0718, respectively. The results of this study can be useful in the design of nanoelectronic, and cooling systems.

Keywords: *Atomistix ToolKit; Density Functional Theory; Single-Walled Boron-Nitride Nanotubes; Single-Walled Carbon Nanotubes; Thermoelectric Properties.*

INTRODUCTION

In recent years, nanostructures have attracted much consideration because of their influential physical, chemical, electrical, biological, and optoelectrical properties. Hence, nanostructures are considered a very good research field [1-2].

Due to their application and properties, carbon nanostructures such as fullerenes, carbon nanotubes (CNTs), and graphene, are among the most important nanostructures. The discovery of CNTs by Sumio Iijima in 1991 was one of the most important developments in the field of nanotechnology [3-5]. These nanostructures are considered suitable options to make changes in many industries. This is due to their special mechanical, electrical, thermal, and optical properties [6].

Because of their one-dimensional electron structures, CNTs can transfer electrons along their length without significant scattering. For example, the mean free path of single-stranded and conductive CNTs is about several microns. As a result, the average means free path can be higher than the length of CNTs, which means ballistic electron transfer and cause a high electrical conductivity [7]. Other important properties of CNTs include good permeability, mechanical,

* Corresponding Author Email: *m.reza.niazian@gmail.com*

and thermal stability, which cause their wide applications in electrical conduction and drug delivery for medical applications [8-11].

Due to the similarity of the h-BN structure to graphene, exploring its properties has been considered by many researchers [12]. Boron nitride structures are compounds of boron (B) and nitrogen (N) atoms with an equal number of atoms, which are arranged in hexagonal, cubic, and crystalline forms. In these structures, B and N located in the same layers are covalently bound. While the atoms located in different layers have the van der Waals interactions. The structure of h-BN is the cause of most of the anisotropies in its properties. The difference in electrical conductivity between h-BN and graphite can be of the order of 10^{18}. The main reason for this is the different electron delocalization in these materials [13-15]. Two methods have been proposed for bulk production of atomically thin BN sheets. One is substrate growth by chemical vapor deposition (CVD) and the other is solution exfoliation under sonication [16-17].

Boron nitride has polymorphs in its crystalline structure with at least 4 different crystallographic forms. Interestingly, carbon bulk also has four similar structures. This is because of the fact that both boron nitride and carbon are isoelectronic materials [18]. In fact, the average number of valence electrons in an atom is the same in these two substances.

BNNTs can be thought of as a rolled BN hexagonal plate. Scientific societies have recently paid more attention to BNNTs than CNTs, caused by the particular properties of BNNTs, including specific mechanical properties, chemical stability, thermal stability, electrical properties, and especially, higher biocompatibility than CNTs. It has been shown that BNNTs have higher biocompatibility and the ability to interact with organic molecules, including proteins and DNA than CNTs. In addition, it has been represented that BNNTs are non-toxic for the cells and do not damage the DNA [19-20]. These properties have made them suitable nanocarriers for medical applications instead of CNTs [21].

Today, due to considerable growth in energy consumption, the management of the energy crisis has found great importance. Hence, thermodynamic materials play an effective role in converting wasted heat into electricity. In this regard, various approaches have been applied including steam and organic Rankine cycle, containing power generation, absorption cooling, direct power generation such as piezoelectric and thermoelectric, biomass locating, desalination, and so on. Among these technologies, thermoelectric is of great importance to recover heat loss. Because, unlike other technologies, it has been converted thermal energy into electrical energy, directly [22].

One of the most interesting approaches in the production and conversion of energy in the future is the Seebeck method, in which thermodynamic materials can be converted directly into electrical energy [23]. Excessive temperature rise can affect the useful life and performance of electronic devices. Therefore, reducing local heat and finding the heat transfer approach is a challenge that should be addressed in future investigations. In this field, one practical method is to use suitable thermodynamic materials with high-temperature performance that can convert heat energy into electricity. Due to their great electrical properties and heat transfer, 2D materials have found applications in thermal management, thermoelectric energy (TE) generation, and heat conversion to electricity [24].In this paper, the thermoelectric properties of the zigzag SWCNT and zigzag SWBNNT with the chirality of (9, 0) are investigated and compared. For this purpose, the first-principle calculations are used.

COMPUTATIONAL MODEL

Figs. 1 and 2 show the configurations of the optimized zigzag SWCNT and zigzag SWBNNT which have been considered for investigation. The first-principle calculations are performed to optimize the geometry of the considered structures and calculate the thermoelectric properties. For this purpose, the DFT is used along with the non-equilibrium Green's function (NEGF) technique. Semi-Empirical (SE) calculator can be used to model the thermoelectric characteristics of molecules, crystals, and devices. For this purpose, self-consistent and non-self-consistent tight-binding models can be employed. Here, tight-binding models are implemented based on Slater–Koster's model [25].In Slater–Koster tight-binding model, the density functional based tight-binding (DFTB) formalism is closely followed, which has been described in. In this model, a numerical function is used to express the distance-dependence of the matrix elements. In the DFTB
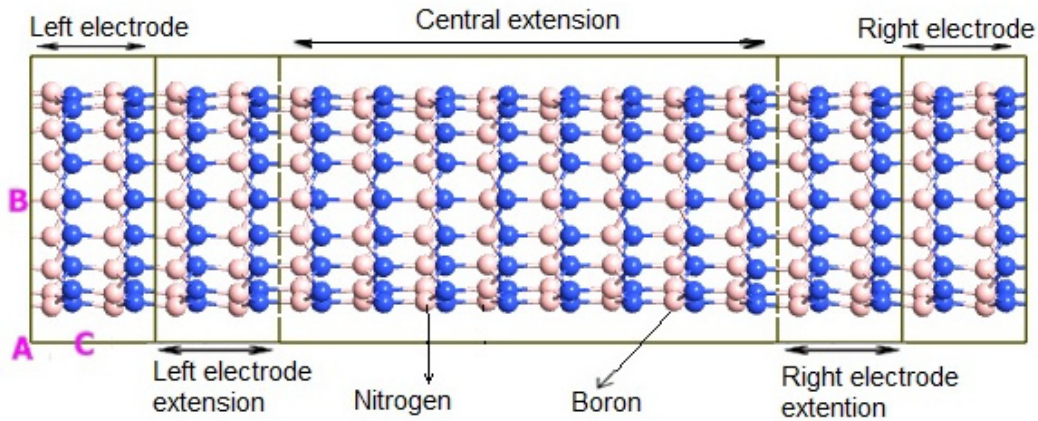
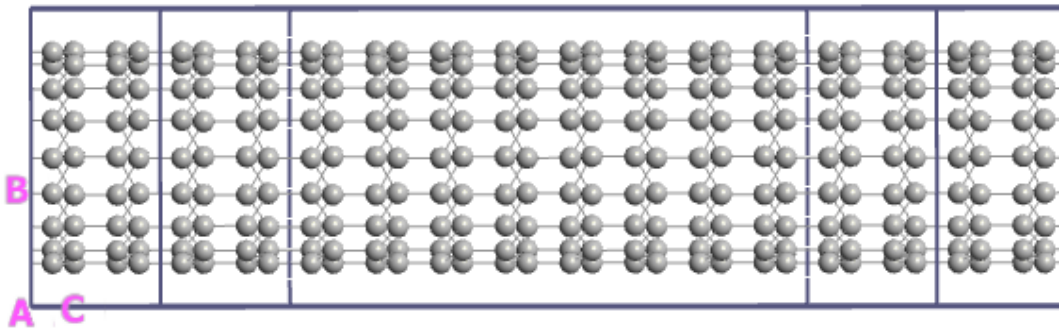Fig.1. Configuration of the optimized zigzag SWBNNT device.

Fig. 2. Configuration of the optimized the zigzag ZSWCNT device.

approach, a second-order expansion of the Kohn-Sham expression of the total energy with respect to the fluctuations of the charge density is used [26-27]. The zeroth-order method is considered a common standard non-self-consistent (TB) plan. While, in the second-order approach, a transparent and parameter-free expression is derived from the elements of the generalized Hamiltonian matrix. Zigzag SWCNT and SWBNNT are considered here as the device and the electrodes with a length of $4.35\,\mathring{A}$ are located at the left and right sides of the devices. Furthermore, the inner tube is selected with the chiralities of $n = 9$, and $m = 0$ which is repeated along the $A = 1$, $B = 1$ and $C = 6$ axes after optimizing the device. The Atomistix ToolKit (ATK) is used for all of the calculations.

Quantum ATK software, formerly known as Atomistix Toolkit and known as ATK software, has unique capabilities for simulating nanostructures and quantum systems at the atomic scale. This software can model the electronic properties of open and closed quantum systems using density-function theory (DFT) using a set of numerical rules for the linear composition of atomic orbitals (LCAO). A key parameter in solving Cohen's equations is the density matrix, which determines the electron density. For open quantum systems, the density matrix is calculated using the Non-equilibrium Green function, abbreviated to NEGF. For alternating and closed quantum systems this matrix is obtained by Hamiltonian diagonalization of Cohen's equations. The electron density then forms a set of effective potentials obtained by Hartree, correlation exchange, and external potential. To depict the atom cores, Troullier–Martins norm-conserving pseudo potentials are employed, which also represent the linear combinations of atomic orbitals and can help to expand the valence states of electrons. The k-point is selected as $1, 1, 150$ in the Brillouin zone and the electrode temperature is set as $T = 300K$. Furthermore, the cutoff energy for
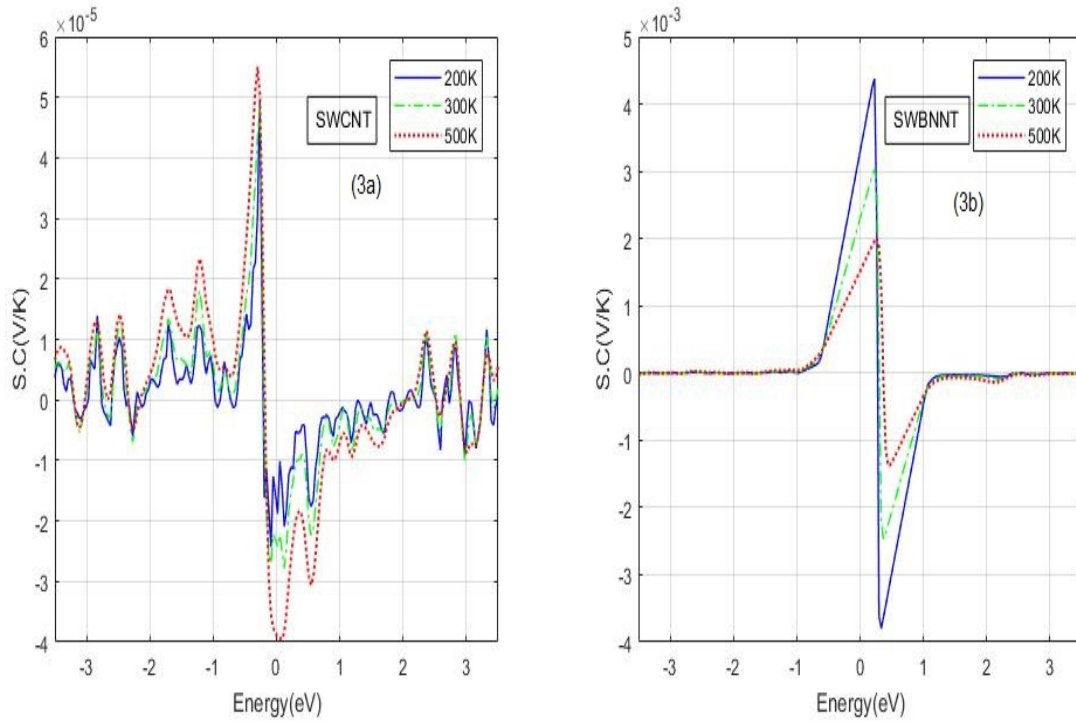
Fig. 3. The Seebeck coefficient spectra in terms of energy of (3a) zigzag SWCNT and (3b) zigzag SWBNNT structure at three different temperatures 200K, 300K and 500K.

the grid integration is considered as $150\,Rydberg$, which is mainly used to control the size of the real space in the partitioning of the integral network and solving Poisson's equation [28-29]. The quasi-Newton approach is utilized for completely optimizing the atomic structures, including the atomic positions as well as the lattice parameters. Besides, the boundary conditions are considered periodic. For all of the simulations, initially, the geometry is optimized until all of the residual forces are smaller than $0.02\frac{eV}{A^\circ}$.

RESULTS AND DISCUSSIONS

Thermoelectric properties

In this section, the thermoelectric properties of the Zigzag SWCNT and Zigzag SWBNNT such as the thermoelectric figure of merit, the Seebeck coefficient, electrons conductance, and thermal conductivity are investigated. For this purpose, three temperatures are considered, including 200K, 300K, and 500K. Applying a temperature difference among the two sides of a material leads to creating a voltage difference which in turn results in an electric current in the material. Furthermore, applying a voltage difference causes the charge carriers (electrons and holes) in the material

to move. Therefore, the electrons move from one side to the other by creating a temperature difference [30- 31].In this way, thermoelectric materials can convert heat directly into electricity and vice versa. The efficiency of a thermoelectric material depends on the thermoelectric figure of merit, known as ZT, which can is expressed by the following relation:

$$ZT = \frac{S^2 G_e T}{K_e + K_l} \quad (1)$$

where S is the Seebeck coefficient, G_e is the electrical conductivity; K_e and K_l are the electronic and lattice contributions, and T is the absolute temperature [32].

Seebeck Coefficient (SC)

In this section, the Seebeck coefficients of the zigzag SWCNT zigzag SWBNNT are investigated. The most common application of the Seebeck effect is in the manufacturing of thermal diodes, thermocouples and electric generators.

The figures (3a) and (3b) show the Seebeck coefficient spectra versus energy of the considered

nanotubes, respectively, at three different temperatures including 200K, 300K and, 500K.

According to relation $\Delta V = S\Delta T$, in which ΔV is voltage difference, S is the Seebeck coefficient, and ΔT is the temperature gradient [33, 21], the temperature difference between the two sides of a material causes the charge carriers to move from the side with the larger temperature (where the electrons have more move) to the side with the smaller temperature (where the electrons have less movement). This movement of electrons results in creating an electric current which causes a voltage difference.

Fig. (3b) shows that the absolute value of the Seebeck coefficient of the zigzag SWBNNT is moderately stable at all of the considered temperatures. The comparison of figure (3a) shows that the Seebeck coefficient of the zigzag SWBNNT decreases by increasing the temperature. In other words, the largest and smallest Seebeck coefficients are observed at the temperature 200K, and 500K, respectively. The results show that the Seebeck coefficient is dependent on temperature and independent of the nanotube structure.

According to the figures (3a) and (3b), the Seebeck coefficient increases by increasing the temperature for Zigzag SWCNT. While it decreases for SWBNNT.

Comparison of Figs. 3a and 3b shows that the peak of the Seebeck coefficient of the SWBNNT is larger than that of the SWCNT. More especially, the peak of the Seebeck coefficient of the zigzag SWCNT at the temperatures of 200K, 300K, and 500K are $4.97 \times 10^{-5} \left(\frac{V}{K}\right)$, $4.88 \times 10^{-5} \left(\frac{V}{K}\right)$, and $5.70 \times 10^{-5} \left(\frac{V}{K}\right)$, respectively. The associated values of SWBNNT are, $4.38 \times 10^{-3} \left(\frac{V}{K}\right)$, $3.03 \times 10^{-3} \left(\frac{V}{K}\right)$ and $2.0 \times 10^{-3} \left(\frac{V}{K}\right)$, respectively.

The results show that at the temperature of 200K, the Seebeck coefficient of SWBNNT is about 88 times that of SWCNT. For a (n, m) SWCNT, if n=m a metallic behavior is observed in the nanotube. Besides, if n - m is a multiple of 3, n≠m and n = m ≠ 0, the nanotube is quasi-metallic with a very small bandgap. Due to the fact that the electric transport coefficient and thermoelectricity are mainly dependent on the electronic properties, a large band gap may reduce the concentration of charge carriers around the Fermi surface [34].

According to the results, the energy gap of zigzag SWCNT is much smaller (0.2 eV) than zigzag SWBNNT (2.6 eV) which can lead to larger Seebeck coefficient in SWBNNT than SWCNT. Comparing zigzag SWCNT and SWBNNT shows that the gap

band length of the SWCNT is much shorter than that of SWBNNT. Hence, it is expected that in the SWBNNT more electrons to be transferred from the valance band to the conductive band by increasing the temperature.

The chemical potential of μ=0 is selected in the highest valence band of these nanostructures, the positive (negative) chemical potential corresponds to the contamination of the charge carrier type n (p).

In addition, when the chemical potential E_F of the zigzag SWCNT and SWBNNT is lower than the Fermi level E_i (i.e. $E_F < E_i$), the Seebeck coefficient S is positive, and when $E_F > E_i$, the Seebeck coefficient is negative. Therefore, it can be concluded that both zigzag SWCNT and SWBNNT are semiconductors and of n-type [35-36].

The Seebeck effect depends on the amount of doping, and the dimension of the sample and the temperature [37].

The electrical conductivity (G_e)

Figs. 4a and 4b show the electrical conductivity spectra (G_e) against the energy of the zigzag SWCNT and SWBNNT, respectively, at the temperatures of 200K, 300K, and, 500K. Fig. 4 indicates that the conductivity experience considerable fluctuations with the change in chemical potential. The changing trend is almost the same at different temperatures, which may be related to the quantum size effect of the zigzag SWCNT and SWBNNT. Figs. 4a and 4b also represent that the electrical conductivity value is almost independent of the temperature. It can be seen that at the temperature of 200K, the maximum amount of electrical conductivities of zigzag SWCNT and SWBNNT are $9.41 \times 10^{-4} S$ and $5.24 \times 10^{-4} S$, respectively.

In addition, in Figs. 4a and 4b an area is observed with a conductivity close to 0 which corresponds to the forbidden band of the zigzag SWBNNT and SWCNT. This area is wider in the zigzag SWBNNT, because the zigzag SWBNNT is a wide-bandgap semiconductor. However, the forbidden band area in SWCNT is very small, which indicates the quasi-conductivity of the nanotube. Therefore, the conductivity of the zigzag SWCNT is expected to be greater than the zigzag SWBNNT. It is also clear from Figs. (4a) and (4b) that the conductivity value is equal at different temperatures. According to these figures, the largest and smallest peaks of the electrical conductivity can be seen in the curves associated with the zigzag SWCNT. Furthermore,
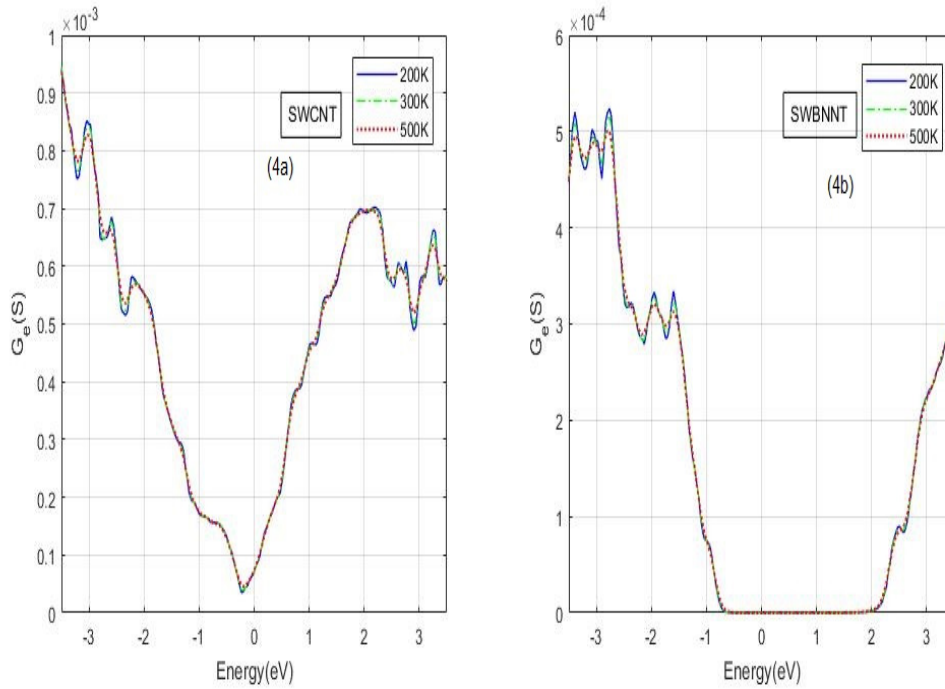
Fig. 4. The conductivity spectra in terms of energy of (4a) zigzag SWCNT and (4b) zigzag SWBNNT structure at three different temperatures 200K, 300K and 500K.
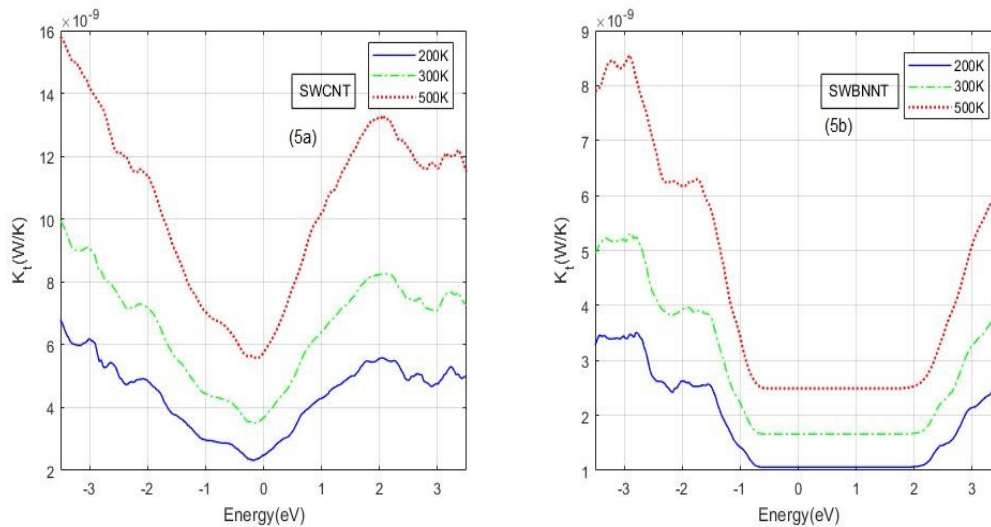

Fig.5. The total thermal conductance spectra in terms of energy of (5a) zigzag SWCNT and (5b) zigzag ZSWBNNT at three different temperatures 200K, 300K and 500K.

the height of conductance peaks are in the range of E < E$_F$ for both of the considered nanotubes. On the other hand, the number of conductance resonances and height of conductance peaks depends on the structure types in the quantum transport that is in accordance with other works [38].

The total thermal conductance (K)

The total thermal conductances ($K_e + K_l$) of the zigzag SWCNT and SWBNNT are also investigated at temperatures 200K, 300K, and 500K. Figs. (5a) and (5b) show the electrons thermal conductance spectra against the energy of the zigzag SWCNT and SWBNNT at the considered temperatures.
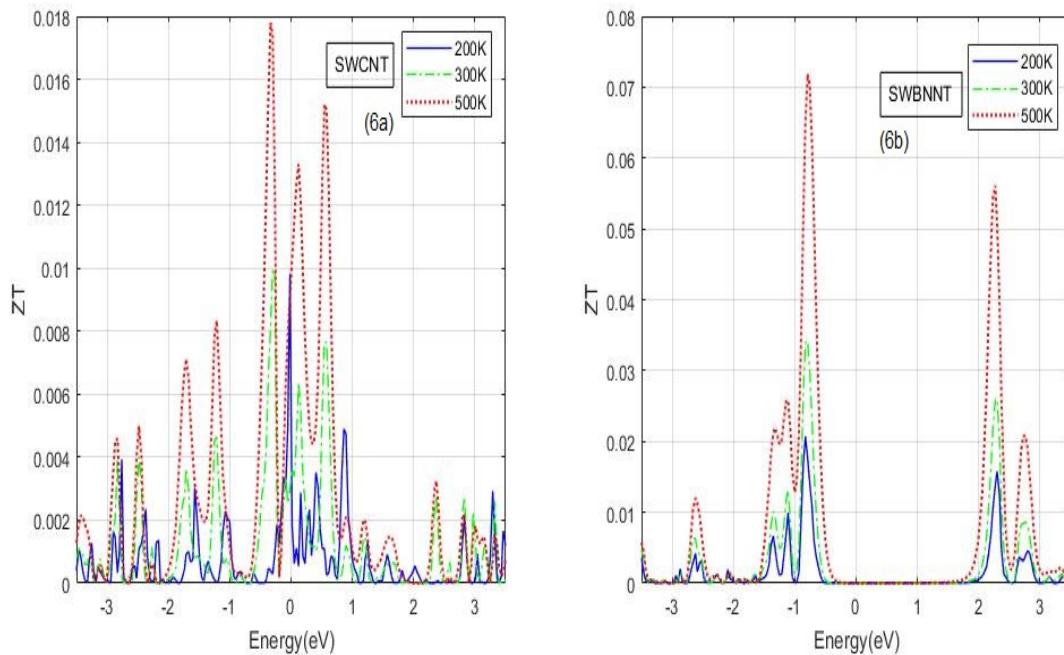
Fig.6. The thermoelectric figure of merit (ZT) spectra in terms of energy of (6a) zigzag SWCNT and (6b) zigzag SWBNNT at three different temperatures 200K, 300K and 500K.

The higher the temperature gradient between the structures in a thermoelectric system, the amount of generating voltage and thermoelectric efficiency of the system is higher. The results show that the total thermal conductance increases with increasing the temperature for both of the structures. In fact, increasing the temperature results in exciting the electrons, besides, many higher-order modes can be excited gradually by increasing the temperature. Hence, thermal conductivity is expected to increase. As the temperature rises, it opens up more channels for phonon transmission [39].

By comparing the changes of K_t values in different bandwidths, it is found that by increasing temperature the K_t of both zigzag SWCNT and SWBNNT increases and the forbidden bandwidth decreases. According to the figures (5a) and (5b), the maximum and minimum peaks of the electrical conductivity are observed for zigzag SWCNT and zigzag SWBNNT, respectively. Also, for both of the zigzag SWCNT and SWBNNT the highest conductivity peaks are in range E < E_F. Due to the anisotropy in the zigzag SWBNNT structure, it is seen that zigzag SWCNT have higher thermal conductivity than zigzag SWCNT.

Thermoelectric figure of merit (ZT)

Efficiency is an important parameter to characterize the thermoelectric properties of nanomaterials. The maximum efficiency of a thermoelectric material is determined by its thermoelectric figure of merit (ZT) [40-42]. The calculated ZTs value as functions of the energy are shown in Figs. (6a) and (6b). As it can be seen, some fluctuations are seen in these figures. Due to the contribution of phonons, the zigzag SWBNNT has larger Seebeck coefficient. the calculations show that the maximum value of ZT of the zigzag SWBNNT at the temperatures of 200K, 300K and, 500K are larger than 0.0207, 0.0342 and, 0.0718, respectively (see Fig. 6a). Furthermore, the maximum value of ZT of the zigzag SWCNT at the temperatures of 200K, 300K and, 500K are larger than 0.0098 ,0.0100 and 0.0178, respectively (see Fig. 6b).

Since the transport coefficients are mainly dependent on the electronic properties, large band gaps may reduce the concentration of charge carriers around the Fermi surface. This can lead to large Seebeck coefficients, as well as large ZT coefficients. At very low temperatures, a small number of electrons are excited, leading

to a decrease in electron thermal conductivity. Therefore, it is possible that thermal conductivity is expressed by the lattice's contribution, meaning that the phonon thermal conduction sentence due to lattice vibrations plays a major role in ZT. As the temperature rises, especially at temperatures above room temperature, more electrons are excited, which leads to an increase in electron conduction, while the lattice contribution decreases due to the increase in phonon scattering due to lattice vibrations.

According to these figures, the value of ZT dramatically decreases in the resonance region of transmission about Fermi's energy. Also, the ZT valsue increases by increasing the temperature for both of the considered nanotubes. The resonant tunneling effect of electron leads to the fluctuations of the electronic conductance. As expected, the maximum of the ZT of the zigzag SWBNNT is larger than zigzag SWCNT, indicating that the thermoelectric properties of the zigzag SWBNNT are better than zigzag SWCNT.

CONCLUSION

In this study, the thermoelectric properties of the zigzag SWCNT and zigzag SWBNNT were investigated at three temperatures including 200K, 300K, and 500K. The structures of the nanotubes were modeled in the Atomistix ToolKit software (ATK). The figure-of-merit (ZT) is an important parameter to determine the thermoelectric properties of nanomaterials. Hence, the ZT value of the zigzag SWCNT and zigzag SWBNNT were evaluated. Because the ZT value depends on some parameters such as the electrical conductivity, the electrons thermal conductance, and Seebeck coefficient, these parameters were also examined. The results showed that the ZT value of the zigzag SWBNNT is larger than the zigzag SWCNT.However, the electrical conductivity, and the electronic and lattice contributions of the zigzag SWBNNT are smaller than those of the zigzag SWCNT.

CONFLICTS OF INTEREST

The authors do not have any conflicts of interest.

REFERENCE

[1] Maslyuk V. V., Achilles S., Sandratskii L., Brandbyge M., Mertig I., (2013), Thermopower switching by magnetic field: First-principles calculations. *Phys. Rev. B*: 88: 081403.

[2] Koumoto K., Mori T., (2013), Thermoelectric nonmaterial's design and applications springier series in materials science. *Springer*, *New York*.

[3] Iijima S., Ichihashi A., (1993), Single-shell carbon nanotubes of 1-nm diameter. *Nature*. 363: 603–605.

[4] Dincer I., Rosen M. A., (1998), A worldwide perspective on energy, environment and sustainable development. *Int. J. Energy Res*. 22: 1305-1321.

[5] Yoshioka S., Hayashi K., Yokoyama A., Saito W., Li H., Takamatsu T., Miyazaki Y., (2020), Crystal structure, electronic structure and thermoelectric properties of β-and γ-Zn 4 Sb3 thermoelectrics: A (3+ 1)-dimensional superspace group approach. *J. Mater. Chem. C.* 8: 9205–9212.

[6] Sheskin A., Schwarz T. , Yu Y., Zhang S., Abdellaoui L., Gault B., Cojocaru-Miredin O., Scheu C., Raabe D., Wuttig M., Amouyal Y., (2018), Tailoring thermoelectric transport properties of Ag-alloyed PbTe: Effects of microstructure evolution. *ACS Appl. Mater. Interf.* 10: 38994-39001 .

[7] Khan I., Saeed K., Khan I., (2019), Nanoparticles: Properties, applications and toxicities. *Arab. J. Chem.*12: 908-931.

[8] He H., Ai Pham-Huy L., Dramou P. , Xiao D., Zuo P., Pham-Huy C., (2013), Carbon nanotubes: Applications in pharmacy and medicine. *Bio. Med. Res. Int.* 12: 578290.

[9] Wakabayashi K., Dutta S., (2012), Nanoscale and edge effect on electronic properties of graphene. *Sci. Rep.* 2: 519-526.

[10] Zuev Y. M., Chang W., Kim P., (2009), Thermoelectric and magnetothermoelectric transport measurements of graphene. *Phys. Rev. Lett.* 102: 096807.

[11] Chang C. P., Lu C. L., Shyu F. L., Chen R. B., Huang Y. C., Lin M. F., (2005), Magnetoelectronic properties of nanographite ribbons. *Phys. E Low-Dimens. Syst. Nanostruc.* 27: 82–97.

[12] Wang J., Ma F., Sun M., (2017), Graphene, hexagonal boron nitride, and their heterostructures: properties and applications. *RSC Adv*. 7: 16801-16806.

[13] Abergel D. S. L., Apalkov V., Berashevich J., Ziegler K., Chakraborty T., (2010), Properties of graphene: A theoretical perspective. *Adv. Phys.* 59: 461-482.

[14] Kane C. L., Mele E., (2005), Quantum spin hall effect in graphene. *J. Phys. Rev. Lett.* 95: 146802-146807.

[15] Walczak K., (2007), Thermoelectric properties of vibrating molecule asymmetrically connected to the electrodes. *Phys. B. Condens. Matter.* 392: 173-179.

[16] Zhou L., Carbotte J. P., (2013), Impact of electron–phonon interaction on dynamic conductivity of gapped dirac fermions: Application to single layer MoS_2. *Phys. B: Condens. Matter.* 421: 97-104.

[17] Sharma V., Kagdada H. L., Jha P. K., Spiewak P., Kurzydłowski K. J.*,* (2020), Thermal transport properties of boron nitride based materials: A review. *Renew. Sustain. Energy Rev.*120: 109622.

[18] Huang L., Zhang Q., Yuan B., Lai X., Yan X., Ren Z., (2016), Recent progress in half-Heusler thermoelectric materials. *Mater. Res. Bullet.* 76: 107-112.

[19] Chen L., Zeng X., Tritt T. M., Poon S. J., (2016), Half-heusler alloys for efficient thermoelectric power conversion. *J. Electron Mater.* 45: 5554–60.

[20] Venkatasubramanian R., Siivola E., Colpitts T., Quinn B., (2001), Thin-film thermoelectric devices with high room-temperature figures of merit. *Nature.* 413: 597–602.

[21] Zevalkink A., Zeier W. G., Pomrehn G., Schechtel E., Tremel W., Snyder G. J., (2012), Thermoelectric properties of Sr3 GaSb3–a chain-forming Zintl compound. *Energy Env. Sci.* 5: 9121-9127.

[22] Kuang W., Hu R., Fan Z. Q., Zhang Z. H., (2019), Spin-dependent carrier mobility and its gate-voltage modifying effects for functionalized single walled black phosphorus tubes. *Nanotechnol.* 30: 145301.

[23] Jiang X., Ban C., Li L., Wang C., Chen W., Liu X., (2021), Thermoelectric properties study on the BN nanoribbons via BoltzTrap first-principles. *AIP Adv.* 11: 055120.

[24] Nasrollahzadeh M., Sajjadi M., Atarod M., Sajjadi S. M., Issaabadi Z., (2019), Types of nanostructures. *Interf. Sci. Technol.* 28: 29-80.

[25] Huang Z., Lu T. Y., Wang H. Q., Yang S. W., Zheng J. C., (2017), Thermoelectric properties of two-dimensional hexagonal indium-VA. *Comput. Mater. Sci*. 130: 232-237.

[26] Kresse G., Furthmuller J., (1996), Efficient iterative schemes for *ab initio* total-energy calculations using a plane-wave basis set. *Phys. Rev. B.* 54: 11169-11175.

[27] Heine T., Seifert G., Fowler P. W., Zerbetto F., (1999), A tight-binding treatment for ^{13}C NMR spectra of fullerenes. *J. Phys. Chem. A.* 103: 8738-8743.

[28] Porezag D., Frauenheim T. H., Köhler T. H., Seifert G., Kaschner R., (1995), Construction of tight-binding-like potentials on the basis of density-functional theory: Application to carbon. *Phys. Rev. B.* 51: 12947-12953.

[29] Carlo A. D., (2002), Tight-binding methods for transport and optical properties in realistic nanostructures. *Phys. B: Condens. Mat.* 314: 211-219.

[30] Deb J., Mondal R., Sarkar U., Sadeghi H., (2021), Electronic and transport property of two-dimensional boron phosphide sheet. *J. Molec. Graph. Model.* 112: 108117-108122**.**

[31] Ding G., Gao G., Yao K., (2015), High-efficient thermoelectric materials: The case of orthorhombic IV-VI compounds. *Sci. Rep.* 5: 9567-9572.

[32] Ma H., Yang C.-L., Wang M.-S., Ma X.-G., (2018), AgKTe: An intrinsic semiconductor material with high thermoelectric properties at room temperature. *J. Alloys Compd.* 739: 35–40.

[33] Niazian M. R., Yaghobi M., (2016), Inelastic electron transport in C$_{70}$ fullerene. *Indian J. Pure & Appl. Phys.* 54: 123-129.

[34] Avouris P., JiaChen J., (2006), Nanotube electronics and optoelectronics. *Mater. Today*. 9: 46-54.

[35] Haque E., Cazorla C., Hossain M. A., (2019), First-principles prediction of large thermoelectric efficiency in superionic Li2 SnX3 (X= S, Se). *Phys. Chem. Chem. Phys.* 22: 878-883.

[36] Yaghobi M., Ramzanpour M. A., Niazian M. R., (2016), Electronic transport through N$_{24}$B$_{24}$ molecular junction. *Chin. J. Chem. Phys.* 29: 223-228.

[37] Boor J. de., Mülle E., (2013), Data analysis for Seebeck coefficient measurements. *Rev. Sci. Inst.* 84: 065102-065107.

[38] Snyder G. J., Snyder A. H., (2017), Figure of merit ZT of a thermoelectric device defined from materials properties. *Energy Environ. Sci.* 10: 2280–2283.

[39] Herrera-Carbajal A., Rodríguez-Lugo V., Hernández-Ávila J., Sánchez-Castillo A., (2021), A theoretical study on the electronic, structural and optical properties of armchair, zigzag and chiral silicon–germanium nanotubes *Phys. Chem. Chem. Phys.* 23: 13075-13086.

[40] Niazian M. R., Matin L. F., Yaghobi M., Masoudi A. A., (2020), Thermoelectric Properties of B12 N12 Molecule. *Current Nanosc.* 16: 936–944.

[41] Pan C., Long M., He J., (2017), Enhanced thermoelectric properties in boron nitride quantum-dot. *Results in Phys.* 7: 1487–1491.

[42] Visan C., (2014), Thermoelectric properties of graphene-boron-nitride nanoribbons with transition metal impurities. *J. Elect. Mater.* 43: 3470–3476.